Mechanics and Mechanical Engineering
Vol. 22, No. 4 (2018) 1015–1030


https://doi.org/10.2478/mme-2018-0081

# Transient Natural Convection in Partitioned Enclosures

Farah Zemani and Amina Sabeur-Bendehina
*Laboratoire des Sciences et Ingénierie Maritimes, Faculté de Génie Mécanique*
*Université des Sciences et de la Technologie d'Oran Mohamed Boudiaf Oran*
*B.P. 1505 Oran El-M'naouar, 31000 Oran, Algérie*
*e-mail: farah.zemani@univ-usto.dz*

Received (29 November 2017)
Revised (10 May 2018)
Accepted (20 November 2018)

In this paper, the natural convection flow in a cavity heated differentially with a partition placed in the middle of the hot wall is numerically simulated. The aspect ratio of the geometry, Prandtl number are fixed at 0.24, 6.64, respectively, for different partitions lengths; however the Rayleigh number values were ranging from $10^6$ to $3.77 \times 10^9$ in order to observe the transition regime. The fluid flow and the heat transfer described in terms of continuity, linear momentum and energy equations were predicted by using the finite volume method. To approach the physical reality experience, calculations were performed in a cavity with the same size and same priority of the fluid with an average temperature $T_m$ imposed on the cooled wall, also another simulation with an average temperature $T_m$ imposed on the horizontal wall.

Time evolution, isotherms and mean Nusselt number are presented for all investigated values. Representative results illustrating the effects of the partition length for the heat transfer and the thermal boundary layer are also reported and discussed. The results indicate that the flow and heat transfer properties are altered by the presence of the partition, especially in the initial stage. In a certain sense, the partition blocks the flow and forces it to come off the hot wall. Since the partition parameters are critical for the transient natural convection flow in the cavity, different partition lengths on the warm wall have been studied.

*Keywords*: natural convection, transient regime, partial partitions, Rayleigh number, Nusselt number, partitions length.

## 1. Introduction

Natural convection in cavities is a subject of major interest because cavities of different fluid-filled geometries are central elements of a long list of engineering and geophysical systems. It is the result of the complex interaction between a thin-sized fluid system in thermal communication with all the walls that confine it.

The problem of natural convection has been studied analytically by Batchelor [1]. Since then, much attention has been given to natural convection in the

cavities. However, De Vahl Davis et al. [2] has focused on the steady natural convection flow in the cavity. Patterson et al. [3] studied unsteady natural convection in a rectangular cavity with instantaneous cooling and heating of two opposite vertical sidewalls. The most important conclusion was that the flow had a strong dependence on the Prandtl number and cavity aspect ratio.The double-structure transition of the thermal boundary layer in a differentially heated cavity has been studied numerically and experimentally by Xu et al. [4,5]. In a first step, the double boundary layer has been described based on experimental results [4]. Xu et al. [5] have focused on the interaction between the inner flow and the thermal boundary layer in the transition process by comparing numerical and experimental results. The mechanism responsible for the formation and evolution of the double structure was discussed by examining the temperature and velocity fields. Previous studies have shown that, depending on wall heating, small disturbances occur near the vertical wall and propagate downstream.

Kolsi et al. [6] has treated the two-dimensional laminar natural convective transient flow characteristics in a differentially heated air-filled tall cavity with gradual heating are investigated both experimentally and numerically for various parameters such as Rayleigh number and temperature difference. Their results showed that as the Rayleigh number increases the flow becomes unstable. Unsteady laminar natural convection of air in a tall cavity was studied numerically by Zhu et al. [7]. Their important result was that the overall Nusselt numbers for the Rayleigh numbers covering the range from $10^3$ to $10^5$ reveals a good agreement with measured data.

Wright et al. [8] investigated a flow visualization of natural convection in a tall air filled vertical cavity using a smoke patterns and interferometers. Experiments results showed that as Ra exceeded $10^4$ the flow became irregular and the core flow became increasingly unsteady. Kumar [9] performed a numerical analysis of the natural convection in a differentially heated cavity, he found that the Nusselt number decreased due to the effect of the thermal conductivity and the increase of the number of Nusselt was more affirmed to the greatest number of Rayleigh.

Additionally to the above-mentioned earlier studies, comprehensive investigations of the natural convection flows in the cavity with a partition on the sidewall have been reported in the recent literature. The effects of the size, material and position of the partitions on the natural convection flows in the cavity have been remunerated much attention. In most of these studies, the thickness of the partition is considered to be sufficiently small in comparison with the fin partition; therefore the fin length is the major geometric parameter for controlling the natural convection flows in the cavity.

Yucel et al. [10] indicated in their numerical analysis of laminar natural convection in filled air enclosures with fins attached to an active wall that with increasing number of fins the heat transfer first reaches a maximum and then approaches a constant, which is not affected by the number of fins. At low Rayleigh numbers, the heat transfer rate increases with the increasing number of fins and the fin length. But, at higher Rayleigh numbers, the heat transfer rate can be decreased or increased by properly choosing the number of fins and the fin lengths.

The transition of the thermal boundary layer from start-up to a quasi-steady state in a side-heated cavity is observed using a shadowgraph technique is also investigated by Xu et al. [11]. A significant feature of the transition revealed from

the present flow visualization is the formation of a double-layer structure along the sidewall at the entrainment development stage. It was believed that the reverse flow in the double-layer structure is the likely cause responsible for the unstable travelling waves at the quasi-steady state. They performed a direct numerical simulation of unsteady natural convection in a differentially heated cavity with a thin fin of different lengths on a sidewall at the Raleigh number of $3.8 \times 10^9$. They found that the fin length significantly impacts on the transient thermal flow around the fin and heat transfer through the finned sidewall in the early stage of the transient flow development.

Frederick et al. [12] investigated in their study that the heat transfer through the finned sidewall is considerably reduced as the fin length increases due to the depression of the natural convection flows adjacent to the finned sidewall.

The transition from a steady to an unsteady flow induced by an adiabatic fin on the side walls was also carried out by Xu et al. [13] they concluded that the fin may induce the transition to an unsteady flow and the critical Rayleigh number for the occurrence of the transition is between $3.72 \times 10^6$ and $3.73 \times 10^6$. Paul et al. [14] treated the effect of an adiabatic fin on natural convection heat transfer in an air filled triangular enclosure by numerical simulations.

Nag et al. [15] carried out numerically the effect on heat transfer of partial horizontal partitions placed on the hot wall of a differentially heated square cavity filled with air for varied width and for varied position along the height axis of the hot wall for Rayleigh numbers ranging from $10^3$ to $10^6$. They suggested a correlation for the average Nusselt number, the Rayleigh number and the width of the horizontal partition for a particular position of the partition along the height. They found that the effect of a horizontal partition is significant.

A numerical study to clarify how presence of a thin fin may affect natural convection heat transfer in a thermally stratified porous layer was undertaken by Zahmatkesh [16]. The most important note of their result was that the natural convection is intensified with decreasing the fin length, moving the fin towards the right wall, decreasing the aspect ratio of the porous layer, and diminishing the stratification parameter concluding that the fin can be used as a control element for natural convection heat transfer in thermally stratified porous layers. Liu et al. [17] conducted experimentally natural convection in a differentially heated water filled cavity with two horizontal adiabatic fins on the sidewalls using the shadowgraph technique. After that a numerical simulation was in a good agreement between the simulation and the experiment.

Oztop et al. [18] also studied numerically a heat transfer in a differentially heated square cavity with cold partition at the bottom wall containing heat generating fluid at Pr=0.71 for Rayleigh numbers characterizing internal and external heating from $10^3$ to $10^6$. Generally, the presence of a cold partition; the heat transfer is reduced and the heat reduction is gradually increased with increasing partition height and thickness. Also the heat transfer is reduced more effectively when the partition is closer to the hot or cold wall. Williamson et al. [19] conducted a numerical study of transition to oscillatory flow in a two dimensional rectangular cavity differentially heated with a conducting partition in the centre, for Rayleigh number ranging from 0.6 to $1.6 \times 10^{10}$ at Prandtl number Pr=7.5. They found that the thermal coupling of the boundary layers on either side of the conducting partition causes flow to

become absolutely unsteady for a Rayleigh number at which otherwise similar non-partitioned cavity flow is steady.

Khatamifar et al. [20] presented some preliminary results on the behavior of boundary layers of conjugated natural convection in a rectangular cavity filled with water with a conductive partition at various locations through a series of experiments and numerical simulations. The experiments were performed for $2.428\times10^9 \leq \mathrm{Ra} \leq 2.458\times10^{10}$ and $5.3701 \leq \mathrm{Pr} \leq 6.1697$, with the partition placed in the center of the cavity. Khanafer et al. [21] studied numerically laminar natural convection heat transfer in a differentially heated square cavity with a thin porous fin attached to the hot wall. The results showed that the presence of the porous fin increases the average Nusselt number for different lengths, positions and angle of inclination of the fin.

Elatar et al. carried out a numerical study of laminar natural convection inside a square enclosure with a horizontal partition attached to its hot wall. They performed a parametric study to learn the effect of the Rayleigh number, the length of the partition, the conductivity ratio, the thickness and the position on the heat transfer. The thickness of the partition showed a negligible effect on the average Nusselt number. It was found that partition efficiency increased in general with increasing partition length. In addition, the efficiency of the maximum partition was found at the lowest Rayleigh number.

Varol et al. [23] did an experimental and numerical study on laminar natural convection in an air filled cavity heated from bottom due to an inclined fin, they observed that the heat transfer can be controlled by attaching an inclined fin onto wall and the presence of inclined fin affects the heat transfer and fluid flow.

Latest, The transition from steady to unsteady coupled thermal boundary layers induced by a finon the partition of a differentially heated cavity filled with water was numerically investigated by Xu [24]. For Rayleigh numbers from $\mathrm{Ra} = 10^7$ to $2 \times 10^{10}$. It has been demonstrated that the fin may induce a transition to unsteady coupled thermal boundary layers and the critical Rayleigh number for the occurrence of the transition is between 3.5 and $3.6 \times 10^8$. It has been found that the flow rate through the cavity with a fin is larger than that without a fin under unsteady flow, indicating that the fin may improve unsteady flow in the partition cavity. Further, The physical mechanism of flow instability and heat transfer of natural convection in a differentially heated water filled cavity with thin fins on the hot wall using the energy gradient theory and the effects of the fin length, the fin position, the fin number, and Ra on heat transfer are investigated numerically by Dou et al. [25]. They found that the effect of the fin length on heat transfer is negligible when Ra is relatively high. When there is only one fin, the most efficient heat transfer rate is achieved as the fin is fixed at the middle height of the cavity. The fins enhance heat transfer gradually with the increase of Rayleigh number under the influence of the thin fins.

The purpose of this investigation is to simulate the unsteady natural convection in a differentially heated cavity with different lengths of partition on the hot wall. The present work is an extension of the work already done by Xu et al. [5] which they treated similar cavity. The side walls are assumed to be differentially heated and the flat top and bottom walls are considered as adiabatic. The thermal and flow behavior and heat transfer characteristics have been studied for various Rayleigh

number and partition lengths. The working fluid media is water with Prandtl number of 6.64 and Rayleigh number ranging from $10^6$ to $3.77 \times 10^9$. The wave features of the thermal flows around the partition are characterized and discussed in this paper.

## 2. Analysis and Modeling

The first simulation concerns the two-dimensional rectangular computational domain and boundary conditions are shown in Fig. 1. The domain which is $H = 0.24\,\mathrm{m}$ high by $L = 1\,\mathrm{m}$ long is considered. One partition is placed in the mid height of the hot wall, the partitions length has been changed $l = L/16$, $L/8$, $L/4$, $L/2$; however, the partition thickness was fixed at $w = H/12$, $T_h = 303.55\,\mathrm{K}$, $T_c = 287.55\,\mathrm{K}$, $T_0 = 295.5\,\mathrm{K}$ and $\Delta T = 16\,\mathrm{K}$. Two other calculations were done respectively.

In the second simulation an average temperature $T_m$ is imposed in the adiabatic walls as shown in Fig. 2 and the third one the temperature of the left horizontal wall is changed to an average temperature $T_m$, Fig. 3 $\left(T_m = \frac{T_h + T_c}{2}\right)$.

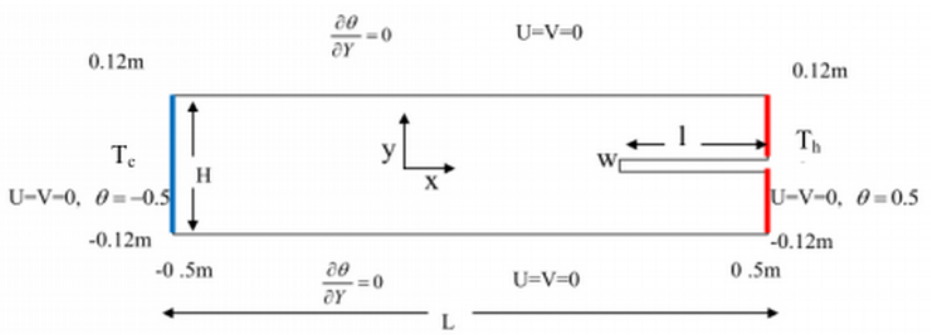


**Figure 1** Computational domain and boundary conditions

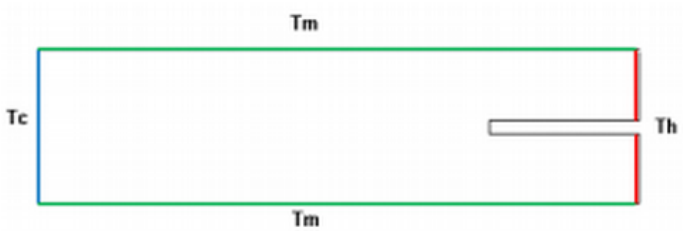


**Figure 2** Schematic diagrams of the physical domain, horizontal walls of temperature $T_m$

The natural convection in the cavity as depicted in all Figures 1, 2 ,3 respectively is described by the differential equations expressing conservation of mass, momentum and energy. The Boussinesq approximation is implemented for the fluid properties to relate density changes to temperature change and to couple in this way the temperature field to the flow field. The governing equations for transient

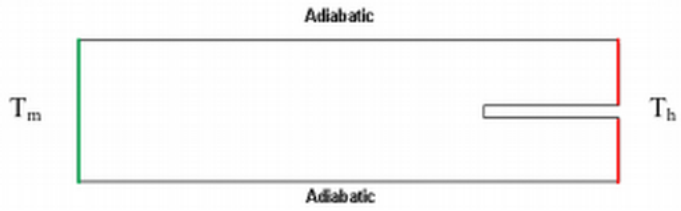


**Figure 3** Schematic diagrams of the physical domain, $\Delta T = 8\,\mathrm{K}$

natural convection can be expressed as follows:

$$\frac{\partial U}{\partial X} + \frac{\partial V}{\partial Y} = 0 \tag{1}$$

$$\frac{\partial U}{\partial \tau} + U\frac{\partial U}{\partial X} + V\frac{\partial V}{\partial Y} = -\frac{\partial P}{\partial X} + \mathrm{Pr}\left(\frac{\partial^2 U}{\partial X^2} + \frac{\partial^2 U}{\partial Y^2}\right) \tag{2}$$

$$\frac{\partial V}{\partial \tau} + U\frac{\partial V}{\partial X} + V\frac{\partial V}{\partial Y} = -\frac{\partial P}{\partial Y} + \mathrm{Pr}\left(\frac{\partial^2 V}{\partial X^2} + \frac{\partial^2 V}{\partial Y^2}\right) + \mathrm{Ra}\,\mathrm{Pr}\,\theta \tag{3}$$

$$\frac{\partial \theta}{\partial \tau} + U\frac{\partial V}{\partial X} + V\frac{\partial V}{\partial Y} = \left(\frac{\partial^2 \theta}{\partial X^2} + \frac{\partial^2 \theta}{\partial Y^2}\right) \tag{4}$$

where :

$$\mathrm{Ra} = \frac{g\beta L^3 \Delta T}{\eta\alpha} \quad \text{and Pr } = \frac{\eta}{\rho} \tag{5}$$

$$\begin{array}{llll} X = \frac{x}{L} & Y = \frac{y}{L} & U = \frac{uL}{\alpha} & V = \frac{vL}{\alpha} \\ P = \frac{pL^2}{\rho\alpha^2} & \theta = \frac{T-T_0}{\Delta T} & \Delta T = T_h - T_0 & \tau = \frac{\alpha t}{L^2} \end{array}$$

The average Nusselt number is defined as follows:

$$Nu = -\int_0^L \frac{h.y}{k} dy \tag{6}$$

## 3. Boundary conditions:

The boundary conditions are no slip for all walls and for energy equation; the side walls have been maintained at differentially heated condition while the other walls are considered as adiabatic. The boundary conditions and the flow domain are shown in Figs. 1, 2 and 3 respectively. They can be written mathematically as non dimensional form:

$$\text{Bottom surface: } U = V = 0, \qquad \frac{\partial \theta}{\partial Y} = 0 \tag{7a}$$

$$\text{Top surface: } U = V = 0, \qquad \frac{\partial \theta}{\partial Y} = 0 \tag{7b}$$

$$\text{Left surface: } U = V = 0, \qquad \theta = -0.5 \tag{7c}$$

$$\text{Right surface: } U = V = 0, \qquad \theta = 0.5 \tag{7d}$$

## 4. Numerical Procedure

The spatial derivatives in the Navier-Stokes equations are discretized with the finite volume method on a staggered grid. The solution domain is covered with finite volumes, having a grid point for a pressure and the temperature in the centre of each volume, grid points for the $u$-velocity in the middle of the west and east side, grid points for the $v$-velocity in the middle of the north and south side of each volume. The equations are integrated over each volume, after which mass, momentum and heat fluxes are discretized with finite differences. The PISO finite volume scheme was used with a second order centre difference scheme approximating the diffusion term, a standard under relaxation technique is enforced in all steps of the computational procedure to ensure adequate convergence. For temporal integration, a Non-Iterative Time-Advancement second order implicit scheme (NITA) was chosen. Calculations are made using time steps $\Delta t = 0.1\,\mathrm{s}$ and $\Delta t = 0.05\,\mathrm{s}$. No difference was distinguished by comparing the temperature fields and the flow for these two time steps.

### 4.1. *Grid*

The quality of the mesh plays an important role in the precision and the stability of the numerical simulations; a non-uniform grid was constructed in the proximity of the partition. Several grids were created for the geometry with partition on the wall in order to test the grid independence. The non-uniform grid system with an expansion factor from the wall surface to the interior is adopted in the boundary layer zones. The rest of the flow domain (the central region of the cavity) is uniformly meshed. The results of the grid dependence test for the case with a partition are illustrated in Fig. 4; the calculated time series of the temperature at point (0.498m, 0.09m) in the early and transitional stage.

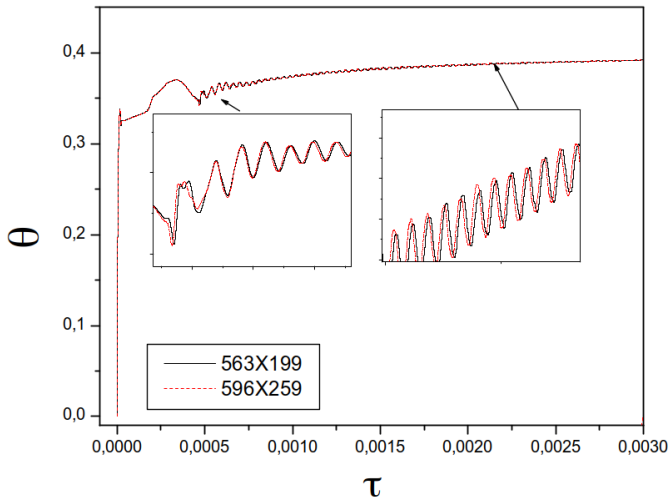


**Figure 4** Temperature time series calculated by using different grids for the case of Ra= $3.77{*}10^9$, and partition length of $L/4$, at the point (0.498, 0.09) plotted

Two meshes of size $563 \times 199$ and $596 \times 259$ for each simulation done (Figure 5) with a non-uniform distribution of points in the $x$ and $y$ directions, the differences between two successive meshes are 1.015 following $x$ and 1.04 following $y$, have been created for the geometry with a partition on the wall to test the independence of the mesh. The Fig. 3 demonstrates the grid distribution adjacent to a partition. Despite strong disturbances due to the presence of the partition on the hot wall, the results calculated using the two meshes are essentially identical. This implies that either of the two finer meshes can be used to resolve the quasi-steady flow in the differentially heated cavity to a high number of Rayleigh $3.77 \times 10^9$.

Good agreement between the current simulation and the literature reported on [5] are obtained, therefore the present numerical procedure may be applied to explore the transient natural convection flows in a differentially heated cavity over a range governing parameters (e.g., different Rayleigh numbers and partition length).

Therefore, in consideration of computing time and precision, the mesh $563 \times 199$ is adopted in the following calculations.

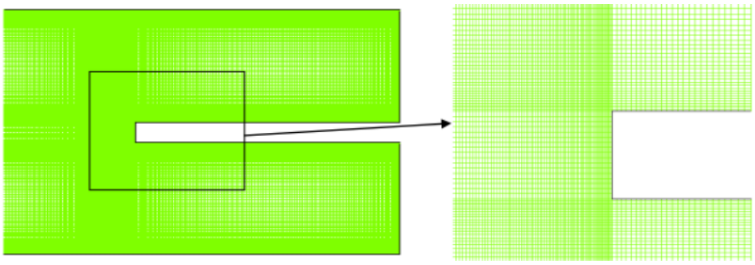

**Figure 5** Grid distribution around the partition

## 5. Results and Discussion

In a differentially heated cavity, the leading edge of the thermal boundary layer (LEE) is the seal of the vertical isothermal sidewall and horizontal adiabatic bottom wall at the upstream corner.The results showed that the development of the vertical thermal boundary layer of the flow with a partition can be classified into three stages: the initial stage, the transient stage and the quasi steady stage.

Figure 4 represents a temporal evolution of the temperature calculated at the point (0.498m, 0.09m) at the linear scale Figure 6 (a) and at the logarithmic scale Figure 6(b) to clearly show the important characteristics of the initial transition of the thermal boundary layer. The flow with the smallest partition has distinct variations in the initial phase. Subsequently, much higher disturbances of the thermal layer induced by the lower intrusion completely outperform the progressive waves as shown in Fig. 4. After the lower intrusion disturbances are summoned, the characteristics of the thermal boundary layer become similar to the case without partition [4, 5]. Basic flow characteristics include separation from intrusion, cold intrusion strike and intrusion oscillations, as shown in Fig. 6.

An important feature of the initial transition of the thermal boundary layer flow is the formation and evolution of lower intrusion. The isotherms of Fig. 6(a)

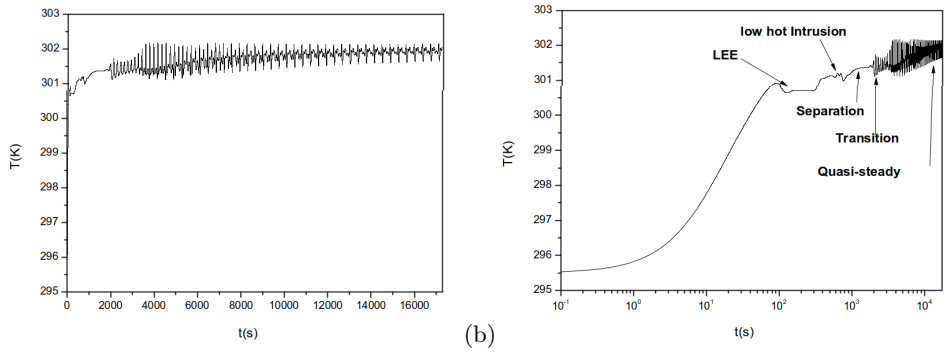


**Figure 6** Temperature versus time, plotted at point (0.498, 0.09) for Ra= $3.77 \times 10^9$ at partition length $l = L/16$: (a) linear time scale; (b) logarithmic time scale

indicate that two intrusions were formed, one under the ceiling and the other under the partition.

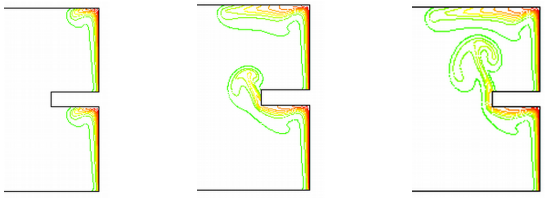

(a) $\tau = 1.4e^{-5}$ (b) $\tau = 2.8e^{-5}$ (c) $\tau = 2.8e^{-5}$

**Figure 7** Isotherms at different moments of initial stage

After the lower intrusion (flow from the lower side hot wall) bypassed the partition, the similarity between the upper and lower sections of the thermal boundary layer disappears Figure 7 (b) and (c).

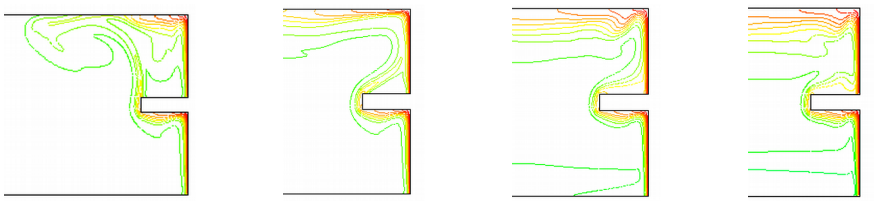

(a) $\tau = 5.6e^{-5}$ (b) $\tau = 9.8e^{-5}$ (c) $\tau = 3.08e^{-4}$ (d) $\tau = 6.3e^{-4}$

**Figure 8** Isotherms at different moments of transient stage

After the lower intrusion has struck the intrusion below the ceiling, it is entrained in the discharged flow and convected remotely, as shown in Fig. 8(a). Figure 8(b) shows the further development of the flow around the partition. Figure 8(c) shows the temperature as the cold intrusion approaches the hot wall. Figure 8(d) shows an upward thermal detachment, and thermal boundary double layer formation.

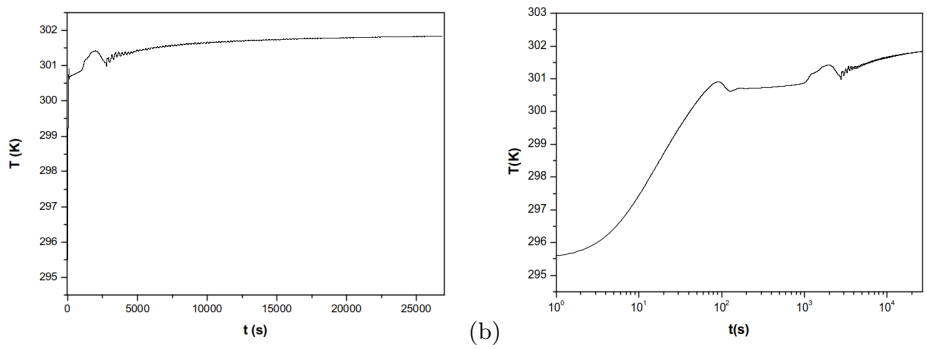


(a) (b)

**Figure 9** Temperature versus time, plotted at point (0.498, 0.09) for Ra $= 3.77 \times 10^9$ at partition length $l = L/4$; (a) linear time scale, (b) logarithmic time scale

To examine transient flows of natural convection let us note the Fig. 9 shows the temporal evolution of the isotherms for the partitioned cavity with the $L/4$ partition. It is clear that disturbances are developed around partitions.

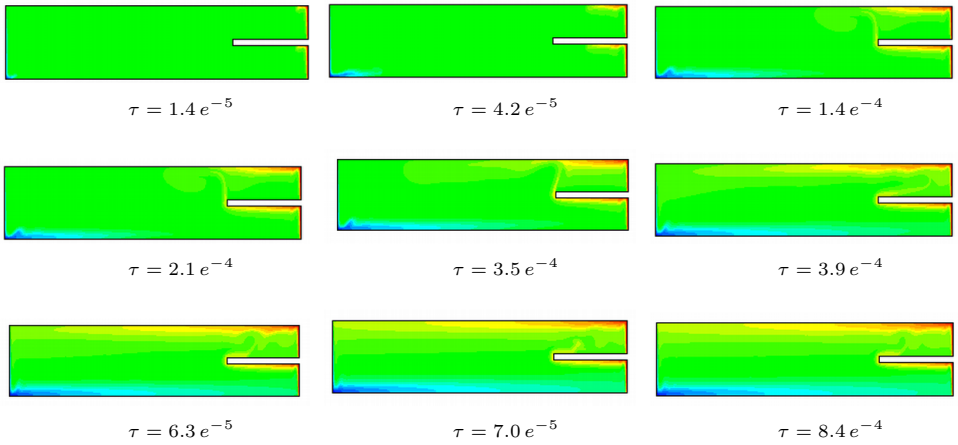


**Figure 10** distribution des isothermes at different moments for $l = L/4$ and Ra$= 3.77 \times 10^9$

Since the partition of this case is longer than the $L/16$ length partition, it takes longer for the lower intrusion to bypass the $L/4$ length partition compared to the $L/16$ length case, Fig. 10.

### 5.1. *Effect of the partition length*

The previous results demonstrated that the flow and heat transfer for both cases show significant variations, indicating that the partition parameter is critical for transient natural convection flow in a differentially heated cavity. Since the $L/4$ length partition can significantly alter the transient natural convection flow in the

cavity, other tests of different partition lengths are performed. Figure 11(a) and (b) illustrate the temporal evolutions of the temperatures calculated at the point ($x = 0.498$, $y = 0.09$) identified in the vertical boundary layer for different lengths of partitions for the high Rayleigh number (Ra= $3.77 \times 10^9$).

This means that the transition from stable to unstable flow occurs as the Rayleigh number increases. It was also noticed that the partition $L/16$ induces more disturbances than the other partitions.

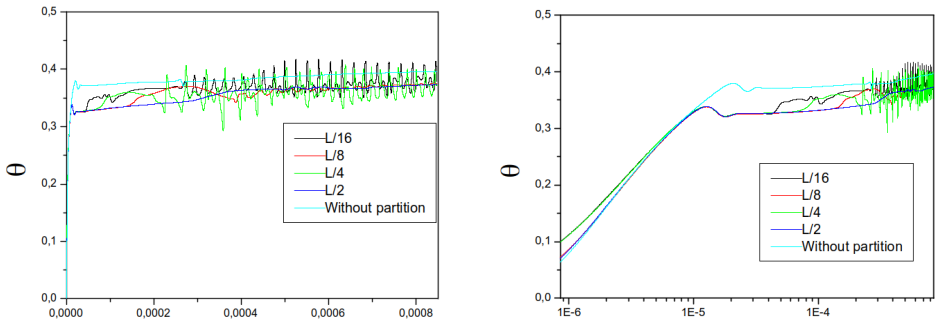


(a) (b)

**Figure 11** Temperature versus time, plotted at point (0.498, 0.09) for Ra= $3.77 \times 10^9$ at different partition lengths: (a) linear time scale (b) logarithmic time scale

As shown in Fig. 11(a) and (b), the size of the partition has a large impact on the characteristics of the temperature wave. The variations of the characteristics of the temperature wave are associated with the variations of the thermal boundary layer flow between the cases with different partitions.

In order to illustrate the flow characteristics of the thermal boundary layer, Figure 12 shows the lower intrusion bypassing the partition at the initial stage for different partition lengths. In the case of the smallest partition, since the lower intrusions are closer to the hot wall after circumventing the partition, the lower intrusion is attached to the downstream wall after the bypass (Figure 12 (a) and (b)). However, for cases with a large partition (c) and (d) show that the lower intrusion development is quite different from that of the smaller partitions.

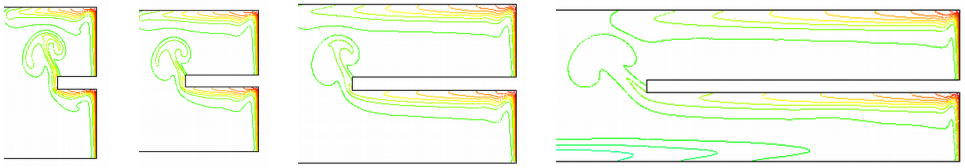

(a) $L/16$ $\tau = 4.2e^{-5}$ (b)$L/8$ $\tau = 6.3e^{-5}$ (c) $L/4$ $\tau = 1.12e^{-4}$ (d) $L/2$ $\tau = 2.24e^{-4}$

**Figure 12** Isotherms for different partition lengths

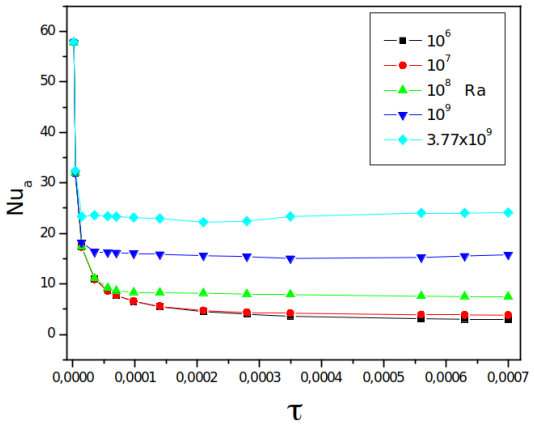


**Figure 13** Mean Nusselt number Nu along the hot wall versus time for different Rayleigh number and for partition length $l = L/4$

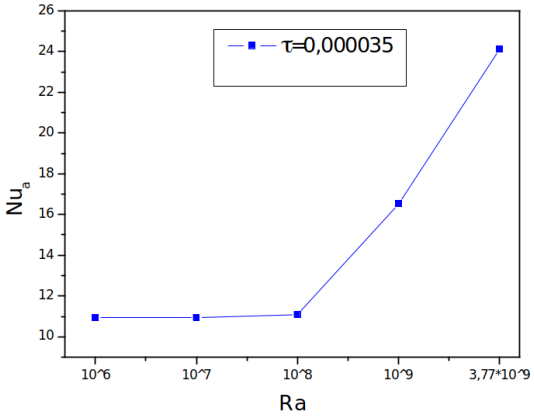


**Figure 14** Numerical results of the Nusselt number according to the Rayleigh number for $L/4$

For the purpose of observing quantitatively natural convection flows and to describe heat transfer through the cavity, the mean Nusselt numbers along the hot partitioned wall versus time was plotted for different Rayleigh numbers value for a length partition of $L/4$. As shown in Fig. 13, the perturbations induced by the oscillation of the thermal flow around the partition have more room to grow. As a consequence, the heat transfer through the partitioned hot wall is notably enhanced so the presence of partition on the hot wall shows a promising result for the enhancement of the heat transfer through a differentially heated cavity. Thus the mean Nusselt number is much smaller near the partition, although oscillatory downstream of the partition. The Nusselt numbers significantly reduce with time in the early stage and then approach an oscillatory state in the cases with and without partition. Also it was noticed at the transitional stage, see Fig. 14, that the average number of Nusselt increases by increasing the number of Rayleigh.

### 5.2. *Horizontal Walls of Temperature* $T_m$

The temperature of the horizontal walls is equal to the average temperature $T_m$, Fig. 3.

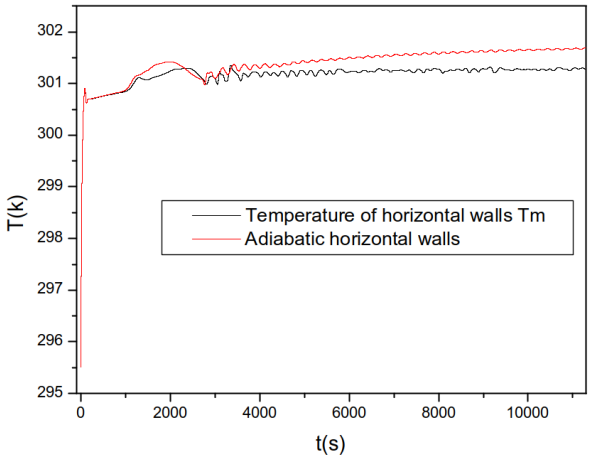


**Figure 15** Temperature time series calculated by using different temperatures of horizontal walls for the case of Ra= $3.77 \times 10^9$, and partition length of $L/4$, polotted at the point (0.498,0.09)

Figure 15 shows a comparison between the cases of adiabatic horizontal wall and horizontal walls with average temperature during the transient regime. The instability of the boundary layer for the average temperature imposed on the horizontal walls gives oscillations more than the adiabatic walls Fig. 16.

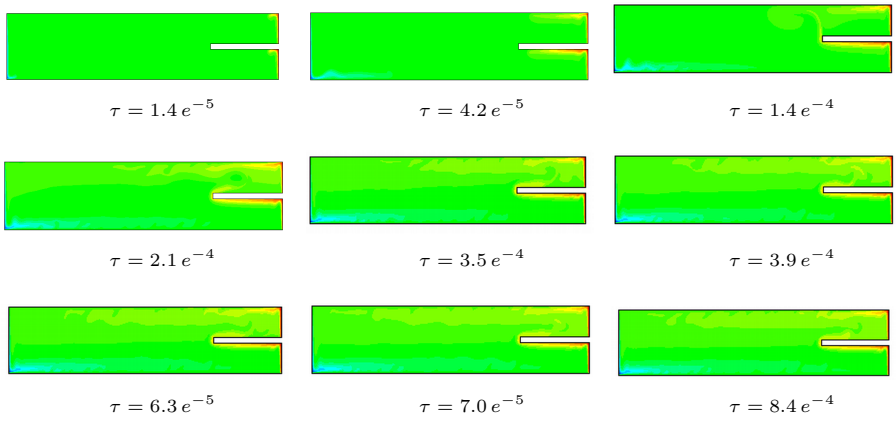


**Figure 16** Isotherms contours at different time for Ra= $3.77 \times 10^9$

### 5.3. *Symmetry of the Flow* $\Delta \mathbf{T} = \mathbf{8}\ \boldsymbol{K}$

Calculations were performed on the same size cavity with the same properties of the fluid. The temperature of the cooled wall is equal to the mean temperature $T_m$ and $\Delta T = 8$ K, Fig. 3.

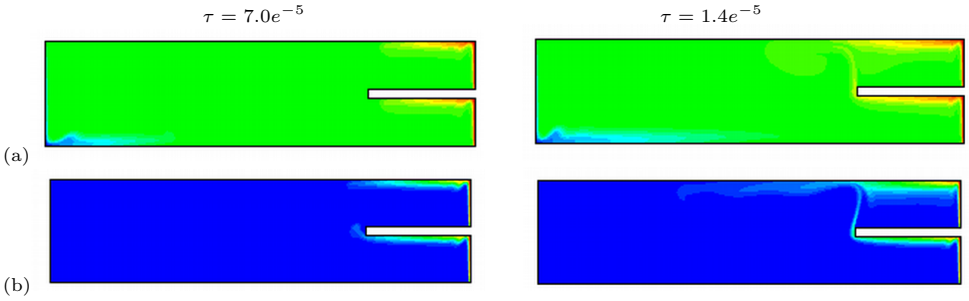


**Figure 17** Comparison of isotherms, for partition length $L/4$ and Ra$= 3.77 \times 10^9$: (a) $\Delta T = 16$ K and (b) $\Delta T = 8$ K

It is noted that the two flows (Fig. 18) in the vicinity of the partitioned hot wall are similar as the cold side has no influence on the hot side.

## 6. Conclusion

In this paper, the natural convection flow in a differentially heated cavity with a partition placed in the middle of the hot wall is simulated numerically. The results indicate that the flow and heat transfer properties are changed by the presence of the partition, especially in the initial stage. In a certain sense, the partition chunks the flow and forces it to come off the hot wall. Because the partition parameters are significant for the transient natural convection flow in the cavity, different partition lengths on the hot wall have been studied.The transition of the natural convection may be classified into three stages: an initial stage, a transitional stage and a quasi steady stage. The numerical results have demonstrated also that the partitions on the hot wall may play an important role in controlling the transient natural convection and heat transfer through a differentially heated cavity in the present Rayleigh number ranging from $10^6$ to $3.77{*}10^9$.

It was also seen that the two flows in the vicinity of the partitioned hot wall are similar in setting the temperature at the cold wall equal to the average temperature, as the cold side has no influence on the hot side, also it was found that the addition of the vertical walls of copper had no influence on the development of the flow due to low wall thickness and high conductivity copper. As well when imposing the temperature at the horizontal walls equal to the average temperature induces perturbation in the flow.

## Nomenclature

| | | | |
|---|---|---|---|
| $g$ | gravitational acceleration [m/s$^2$] | $U$ | velocity component in $x$ dir. [m/s] |
| $h$ | convective heat transfer coeff. [W/m$^2$ K] | $V$ | velocity component in $y$ dir. [m/s] |
| $H$ | height of the enclosure [m] | W | partition thickness |
| $l$ | partition length [m] | x, y | Cartesian coordinates [m] |
| $L$ | width of the enclosure [m] | Greek symbols | |
| Nu | Nusselt number | $\tau$ | dimensionless time |
| $p$ | pressure [N/m$^2$] | $k$ | thermal conductivity of fluid [W/m K] |
| Pr | Prandtl number | $\alpha$ | thermal diffusivity [m$^2$/s] |
| Ra | Rayleigh number | $\beta$ | coeff. of volumetric expansion [1/K] |
| $T$ | temperature [K] | $\mu$ | dynamic viscosity [N s/m$^2$] |
| $T_h$ | temperature of the hot surface [K] | $\rho$ | fluid density [kg/m$^3$] |
| $T_c$ | temperature of the cold surface [K] | Subscripts | |
| $T_0$ | initial temperature [K] | C | Cold |
| $T_m$ | average temperature [K] | H | Hot |
| $\Delta T$ | Temperature variation, $T_h - T_c$ [K] | 0 | Initial |
| | | m | mean |

## Acknowledgements

The authors are immensely grateful to the reviewers for their comments on an earlier version of the manuscript.

## References

[1] **Bachelor G.K.**: Heat transfer by free convection across a closed cavity between vertical boundaries at different temperatures *Quart. Appl. Math.*, **12**, 209–233, **1954**.

[2] **De Vahl Davis, G.**: Natural convection of air in a square cavity: a bench mark numerical solution, *Int. J. Numer. Meth. Fluids*, **3**, 249–264, **1983**.

[3] **Patterson, J.C., Armfield, S.W.**: Transient features of natural convection in a cavity, *J. Fluid Mech.*, **219**, 469–497, **1990**.

[4] **Xu.F, Patterson,J.C. Lei. C.**: Shadowgraph observations of the transition of the thermal boundary layer in a side-heated cavity, *Experiments in Fluids*, **38**, 770–779, **2005**. DOI: 10.1007/s00348-005-0960-1.

[5] **Xu, F., Patterson, J.C., Lei, C.**: *Transient of thermal boundary layer in a differentially heated cavity to a double layer structure*, James Cook University, Australia, **2005**.

[6] **Kolsi.L., Ben Hamida M.B., Hassen, W., KadhimHussein, A., Borjini, M.N., Sivasankaran, S., Saha, S.C., Awad, M.M., Fathinia, F., Ben Aissia, H.**: Experimental and Numerical Investigations of Transient Natural Convection in Differentially Heated Air-Filled Tall Cavity, *American Journal of Modern Energy*, 30–43, **2015**. DOI: 10.11648j.ajme.20150102.12.

[7] **Zhu, Z.J., Yang, H.X.**: Numerical investigation of transient laminar natural convection of air in a tall cavity, *Heat and Mass Transfer*, **39**, 579–587, **2003**. DOI: 0.1007/s00231-002-0385-9.

[8] **Wright, J.L., Jin, H., Hollands, K.G.T., Naylor, D.**: Flow Visualization of Natural Convection in a Tall, Air-Filled Vertical Cavity, *J. Heat Mass Transfer*, **2005**. DOI: 10.1016/J.heat mass transfer.06.045.

[9] **Kumar, A., Baig, M. and Asrar, W.**: Evolution to chaotic natural convection in a rectangular enclosure with mixed boundary conditions, *Numerical Heat Transfer, Part A: Applications*, **34**, 447–462, **1998**.

[10] **Yucel. N., Turkoglu, H.**: Numerical analysis of laminar natural convection in enclosures with fins attached to an active wall, *Heat and Mass Transfer*, **33**, 307–314, **1998**.

[11] **Xu, F., Patterson, J.C., Lei, C.**: Transient Natural Convection in a Differentially Heated Cavity with a Thin Fin of Different Lengths on a Sidewall, 16th Australasian Fluid Mechanics Conference, **2011**.

[12] **Frederick, R.L.**: Natural convection in an inclined square enclosure with a partition attached to its cold wall, *Int. J. Heat Mass Transfer*, **32**, 87–94, **1989**.

[13] **Xu, F., Saha, S.V.**: Transition to an unsteady flow induced by a fin on the sidewall of a differentially heated air filled square cavity, *International Journal of Heat and mass Transfer*, **71**, 236–244, **2014**.

[14] **Paul, S.C., Saha, S.C, Gu, Y.T.**: Effect of an adiabatic fin on natural convection heat transfer in a triangular enclosure, *American Journal of Applied Mathematics*, **1**(4), 78–83, **2013**. DOI: 0.11648,0104.16.

[15] **Zahmatkesh, I.**: On the importance of thermal boundary conditions in heat transfer and entropy generation for natural convection inside a porous enclosure, *International Journal of Thermal Sciences*, **47**, 339–346, **2008**.

[16] **Liu. Y., Lei. C., Patterson, J.C.**: Natural convection in a differentially heated cavity with two horizontal adiabatic fins on the sidewalls, *International Journal of Heat and Mass Transfer*, **72**, 23–36, **2014**.

[17] **Oztop, H., Bilgen, E.**: Natural convection in differentially heated and partially divided square cavities with internal heat generation, *International Journal of Heat and Fluid Flow*, **27**, 466–475, **2006**.

[18] **Williamson, N., Armfield, S.W., Kirkpatrick M.P.**: Transition to oscillatory flow in a differentially heated cavity with a conducting partition, *J. Fluid Mech.*, **693**, 93–111, **2012**. DOI: 10.1017/jfm.2011.471.

[19] **Ambarita, H., Kishinami, K., Daimaruya, M., Saitoh, T., Takahashi, H., Suzuki, J.**: Laminar natural convection heat transfer in an air filled square cavity with two insulated baffles attached to its horizontal walls, *Thermal Science and Engineering*, **14**(3), **2006**.

[20] **Khatamifar, M., D'Urso, R., Lin, W., Holmes, D., Armfield, S.W., Kirkpatrick, M.P.**: A numerical and experimental study on the unsteady conjugate natural convection, boundary layers in a water filled rectangular cavity with a conducting partition wall at varied locations, 19th Australasian Fluid Mechanics Conference Melbourne, **2014**.

[21] **Khanafer, K., AlAmiri, A., Bull, J.**: Laminar natural convection heat transfer in a differentially heated cavity with a thin porous fin attached to the hot wall, *International Journal of Heat and Mass Transfer*, **87**, 59–70, **2015**.

[22] **Elatar, A., Teamah, M.A., Hassab, M.A.**: Numerical study of laminar natural convection inside square enclosure with single horizontal fin, *International Journal of Thermal Sciences*, **99**, 41–51, **2016**.

[23] **Varol, Y., Oztop, H.F., Ozgen, F., Koca, A.**: Experimental and numerical study on laminar natural convection in a cavity heated from bottom due to an inclined fin, *Heat Mass Transfer*, **48**, 61–70, **2012**. DOI: 10.1007/s00231-011-0843-3.

[24] **Xu, F.**: Unsteady coupled thermal boundary layers induced by a fin on the partition of a differentially heated cavity, *International Communications in Heat and Mass Transfer*, **67**, 59–65, **2015**.

[25] **Dou, H.S., Jiang, G.**: Numerical simulation of flow instability and heat transfer of natural convection in a differentially heated cavity, *International Journal of Heat and Mass Transfer*, **103**, 370–381, **2016**.